REPORT DOCUMENTATION PAGE

Form Approved
OMB NO. 0704-0188

1. AGENCY USE ONLY (Leave Blank)	2. REPORT DATE	3. REPORT TYPE AND DATES COVERED
		Reprint

4. TITLE AND SUBTITLE
Mutual Effects of Hydrogenation and Deformation in Ti-Nb Alloys

5. FUNDING NUMBERS
DAAD19-01-1-0377

6. AUTHOR(S)
See attached report

7. PERFORMING ORGANIZATION NAME(S) AND ADDRESS(ES)
Colorado School of Mines
1500 Illinois St.
Golden CO 80401-1890

8. PERFORMING ORGANIZATION REPORT NUMBER

9. SPONSORING / MONITORING AGENCY NAME(S) AND ADDRESS(ES)

U. S. Army Research Office
P.O. Box 12211
Research Triangle Park, NC 27709-2211

10. SPONSORING / MONITORING AGENCY REPORT NUMBER

41922.6-MS

11. SUPPLEMENTARY NOTES
The views, opinions and/or findings contained in this report are those of the author(s) and should not be construed as an official Department of the Army position, policy or decision, unless so designated by other documentation.

12 a. DISTRIBUTION / AVAILABILITY STATEMENT	12 b. DISTRIBUTION CODE
Approved for public release; distribution unlimited.	

13. ABSTRACT (Maximum 200 words)

See Attached Report

14. SUBJECT TERMS	15. NUMBER OF PAGES
	16. PRICE CODE

17. SECURITY CLASSIFICATION OR REPORT	18. SECURITY CLASSIFICATION ON THIS PAGE	19. SECURITY CLASSIFICATION OF ABSTRACT	20. LIMITATION OF ABSTRACT
UNCLASSIFIED	UNCLASSIFIED	UNCLASSIFIED	UL

Mutual Effects of Hydrogenation and Deformation in Ti-Nb Alloys

D. ZANDER, D.L. OLSON, and D. ELIEZER

Alloying of Ti-based alloys with hydrogen is used to modify the microstructure and improve mechanical properties. In this study, hydrogen charging was performed electrochemically in a 2:1 glycerin-phosphoric acid electrolyte at high fugacities. This research investigated in detail, by means of X-ray diffraction, scanning electron microscopy (SEM), transmission electron microscopy (TEM), thermal desorption spectroscopy (TDS), and microhardness tests, the influence of hydrogen at high fugacities on the phase stability, desorption behavior, and microhardness in Ti-Nb (20 to 45 wt pct Nb) alloys before and after deformation. Hydrogenation of Ti-Nb was found to exhibit a significant effect on the phase stability as well as the microhardness of Ti-Nb alloys. Hydrogenation of Ti-20 wt pct Nb led to precipitation of $(Ti,Nb)H_x$ in the metastable α'' matrix. In Ti-Nb alloys with 40 or 45 wt pct niobium, hydrogen stabilized the bcc β phase, but destabilized the hcp ω phase. With increasing hydrogen content, an expansion of the lattice constant of the β phase occurred, followed by the formation of $(Ti,Nb)H_x$. The influence of hydrogen on the microhardness of Ti-40 wt pct Nb and Ti-45 wt pct Nb shows only a minor effect, whereas Ti-20 wt pct Nb exhibits significant softening in response to hydrogen charging up to 3000 ppm. The TDS showed that deuterium desorption strongly depends on the niobium content and the deformation treatment prior to or after charging. The observed results should provide further insight on the mutual effects and the resulting micromechanism of hydrogenation and deformation in Ti-Nb alloys.

I. INTRODUCTION

THE wide spectrum for application of titanium and its alloys has necessitated adjusting their mechanical properties to the appropriate structural needs. The microstructure of α-and β-type titanium alloys has a dominating influence on the tensile strength, fatigue properties, and fracture toughness. Historically, thermomechanical processing and heat treatment were used to control microstructural properties in titanium alloys,[1] but more recently, thermochemical processing (TCP)[2–5] has become the more important technique in improving processing, as well as the mechanical properties of these alloys.

The design of Ti-based alloys can be made more efficient through the use of hydrogen as a temporary alloying element, since both manufacturing temperatures and stresses can be decreased. Early work using hydrogen-assisted processing in Ti-based alloys demonstrated that hydrogen could lead to improved workability.[6,7,8] Titanium and conventional Ti-based alloys have a high solubility for hydrogen. The Ti-H system is of a eutectoid type and consists of several hydride phases of the hcp α phase and the bcc β phase: two interstitial solid solutions of hydrogen based on the allotropic α and β forms of pure titanium.[9] The β-titanium alloys have even lower activity values than commercially pure titanium and a consequently higher hydrogen solubility.[4] In addition, in refractory metals or alloys, hydrogen has a large potential to promote superplasticity. It is also known that in bcc metals, *e.g.*, in iron,[10] hydrogen enhances plasticity at temperatures between 200 and 300 K, because segregation of hydrogen at dislocations lowers their stress field.

Ti-Nb alloys have been produced for use in, *e.g.*, the aerospace industry, nuclear industry, and for superconducting applications. New developments are going in the direction of medical applications, *e.g.*, as surgical implants, because of their good mechanical and chemical properties. Until now, some work has been conducted on the processing and mechanical behavior of Ti-Nb alloys, but very few results are known about the nonequilibrium conditions of phase transformations in Ti-Nb alloys due to hydrogen charging at high fugacities. Popov *et al.*[11,12] reported that gaseous hydrogenation at 800 °C leads to considerable changes in the stability range of the different phases, and they published a metastable phase diagram of quenched Ti-Nb-H alloys containing up to 33 at. pct niobium and up to 25 at. pct hydrogen. In the same study, the authors also noted that stabilization of a metastable β phase could be achieved with a hydrogen content above 10 at. pct. The purpose of our present research is to investigate the hydrogenation/deformation aspects of TCP in Ti-Nb alloys in detail: the influence of hydrogen on phase stability, thermal desorption, and microhardness; and the influence of hydrogen on thermal desorption prior to or after deformation in sintered Ti-20 wt pct Nb and Ti-40 wt pct Nb alloys as well as in commercial Ti-45 wt pct Nb.

II. EXPERIMENTAL PROCEDURE

The investigations were performed on sintered Ti-20 wt pct Nb and Ti-40 wt pct Nb alloys as well as on

D. ZANDER, Assistant Professor, is with the Department of Chemical Engineering University of Dortmund, D-44221 Dortmund, Germany. Contact e-mail: daniela.zander@ct.uni-dortmund.de D.L. OLSON, Professor, is with the Department of Metallurgical and Materials Engineering, Colorado School of Mines, Golden, CO 80401-1887. D. ELIEZER, Professor, is with the Department of Materials Engineering, Ben Gurion University of the Negev, Beer-Sheva 84105, Israel.

This article is based on a presentation made in the symposium entitled "Fundamentals of Structural Intermetallics," presented at the 2002 TMS Annual Meeting, February 21-27, 2002, in Seattle, Washington, under the auspices of the ASM and TMS Joint Committee on Mechanical Behavior of Materials.

a commercial Ti-45 wt pct Nb alloy. The consolidation process for the sintered Ti-Nb powders was carried out at 30 kbar, followed by annealing for 12 hours at 1000 °C. Afterward, Ti-20 wt pct Nb was homogenized for 1 hour at 1100 °C, and Ti-40 wt pct Nb was homogenized for 1 hour at 1300 °C. The microstructure and phase stability were studied by X-ray diffraction (Cu Kα radiation); optical microscopy; scanning electron microscopy (SEM), using a JEOL* JSM-5600; and transmission electron microscopy (TEM), using a FasTEM JEOL 2010. For optical microscopy and SEM studies, polished specimens were slightly etched with a 2 HF:1 HNO_3:17 H_2O solution.

*JEOL is a trademark of Japan Electron Optics Ltd., Tokyo.

For TEM, the specimens were thinned by ion polishing (Gatan-pips 691) as well as by electrochemical polishing in a solution of perchloric acid, n-butanol, and methanol (1:6:10). Two preparation methods were used to exclude phase transformation due to preparation effects.

After grinding, the investigated Ti-Nb alloys were electrolytically charged with hydrogen in a 2:1 glycerine–phosphoric acid electrolyte at 25 °C and a current density of $i = 500$ A/m^2. The hydrogen content was measured by a LECO* apparatus.

*LECO is a trademark of LECO Corporation, St. Joseph, MI.

Deuterium desorption of hydrogenated Ti-Nb was measured by thermal desorption spectroscopy (TDS) with a heating rate of 5 K/min. The TDS technique is a very sensitive one for studying trapping[13,14,15] and diffusion processes[16] in, for example, crystalline materials. The technique involves measurements of the desorption rate of hydrogen or deuterium, soluted or trapped in the material, while heating the sample. Further experimental details are given elsewhere.[13] The influence of hydrogen on the microhardness of the Ti-Nb alloys was investigated at room temperature using a Matsuzaura MHT-1 microhardness tester. For microhardness measurements, the specimens were mounted in epoxy and polished metallographically (up to 0.05 μm).

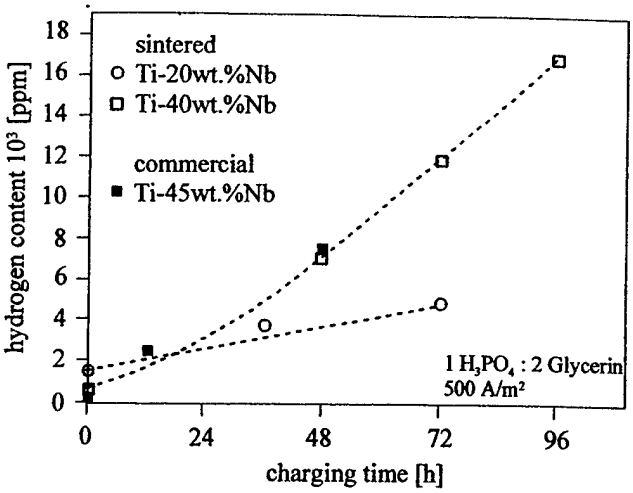

Fig. 1—Hydrogen content of Ti-Nb alloys after charging at high fugacities.

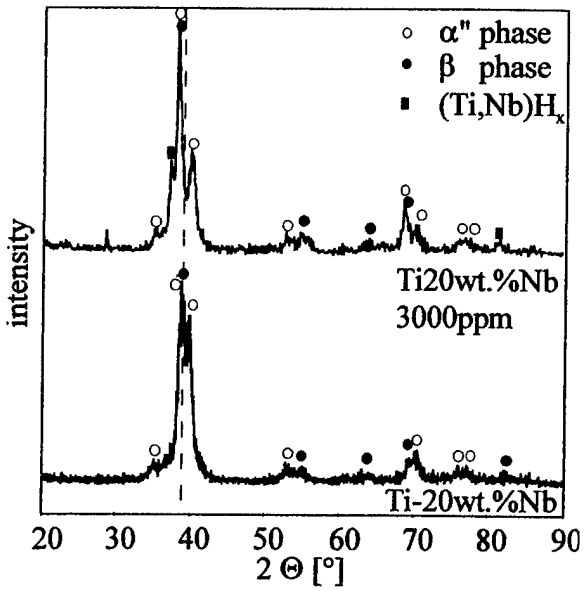

Fig. 2—X-ray diffraction of Ti-20 wt pct Nb before and after hydrogenation for 24 h at 500 A/m^2.

III. RESULTS

A. *Effect of Hydrogen on Microstructure and Phase Transformations*

Figure 1 shows the hydrogen content of Ti-Nb alloys after charging at high fugacities. The hydrogen storage capacity was found to be higher and the kinetics to be faster for sintered Ti-40 wt pct Nb and commercial Ti-45 wt pct Nb than for sintered Ti-20 wt pct Nb during hydrogenation at 500 A/ m^2 for up to 72 hours.

Microstructural investigations, *i.e.*, optical microscopy, SEM, and TEM (Figure 3(a)) of sintered Ti-20 wt pct Nb showed a martensitic structure with some long, relatively thick primary martensite plates and a large number of secondary plates. It was reported[17] that the volume fraction of martensite in Ti-Nb alloys depends on the niobium concentration as well as the interstitial content. While the size and volume fraction of the large plates decreased with increasing niobium content, the higher-interstitial-content alloys, at a constant niobium concentration, exhibited an increased volume fraction of martensite plates.

Extensive examination of phase equilibria in Ti-Nb alloys have shown that the α (hcp) and β (bcc) are the low-temperature stable phases. Quenching the β phase from elevated temperatures can result in the formation of two metastable martensite structures, α' (hexagonal) and α'' (orthorhombic).[18] The α' is observed in alloys containing less than 13 wt pct niobium, whereas alloys containing more than a 13 wt pct niobium content transform into α'' martensite.[19] It might be that the α'' phase can be seen as a transitional phase between the α' hexagonal structure and the β bcc structure.A comparison[17] of microstructure studies involving alloys of compositions between 25 and 50 wt pct niobium indicates that, in addition to the composition, changes in either the cooling rate or total interstitial content can also result in different microstructures. The X-ray diffraction of the investigated Ti-20 wt pct Nb (Figure 2)

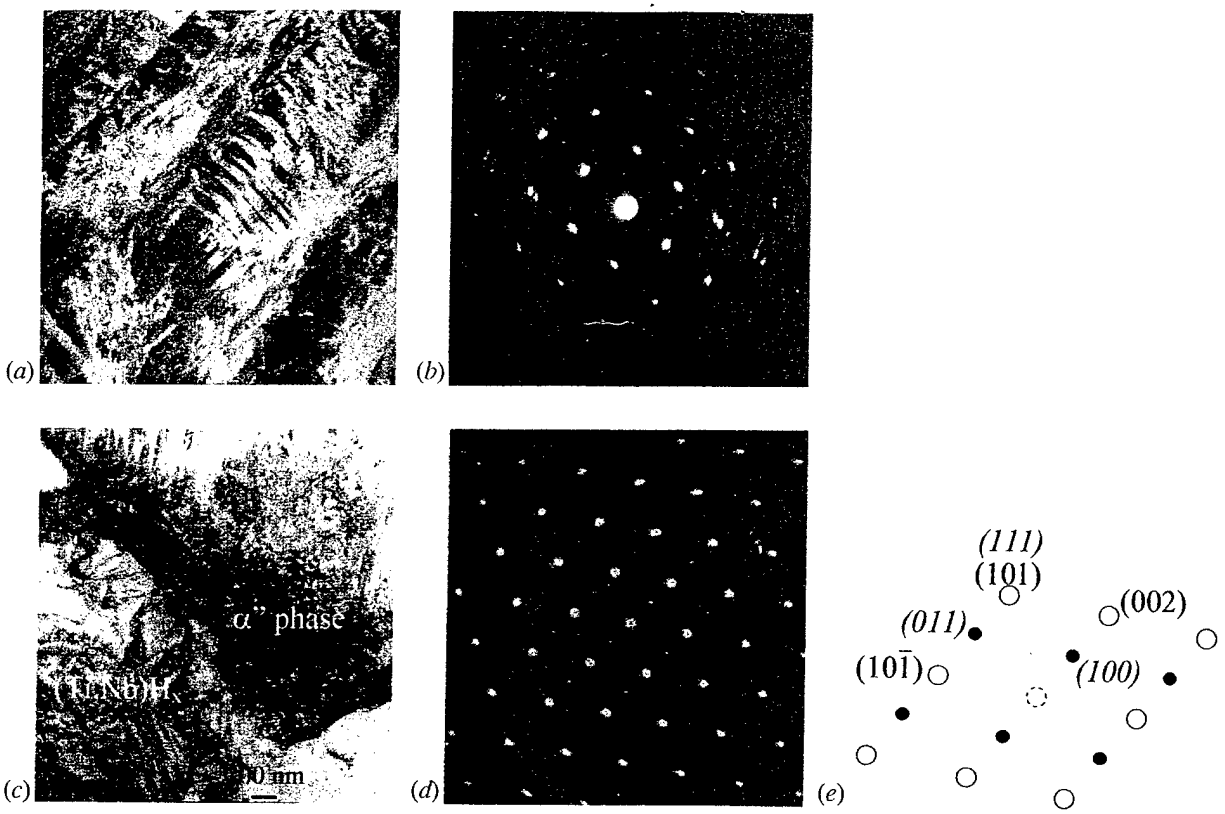

Fig. 3—Influence of hydrogenation on the microstructure of Ti-20 wt pct Nb: (*a*) TEM of the sintered alloy, (*b*) corresponding electron diffraction pattern of the orthorhombic α'' phase, (*c*) TEM of the hydrogenated alloy (500 A/m^2, 24 h), (*d*) the α'' matrix and (Ti,Nb)H_x, and (*e*) index scheme of the electron diffraction of α'' matrix (○) and (Ti,Nb)H_x(●).

indicated that the martensitic phase can be indexed with the hcp α phase (a = 0.295 nm and c = 0.468 nm) or the orthorhombic α'' phase (a = 0.299 nm, b = 0.509 nm, and c = 0.468 nm) and the bcc β phase (a = 0.331 nm). The broadening of the X-ray diffraction peaks can be attributed to high-stress fields. The TEM diffraction (Figure 3(b)) confirmed the formation of the orthorhombic α'' phase with the lattice parameters a = 0.299 nm, b = 0.509 nm, and c = 0.468 nm.

The X-ray diffraction (Figure 2) of sintered Ti-20 wt pct Nb, consisting of the α'' and the bcc β phase hydrogenated for 24 hours at high fugacities, revealed the formation of (Ti,Nb)H_x. The intensities of the X-ray peaks of the β phase are much higher and less diffuse after electrochemical hydrogenation than before charging. The X-ray diffraction also indicated that the lattice parameter of the retained β phase increases during hydrogenation. This behavior can be explained by the expansion of the lattice due to the dissolved hydrogen atoms which randomly occupied the interstitial sites of the bcc unit cell and is consistent with the high solubility of hydrogen in the β phase.

The TEM investigations (Figure 3) of Ti-20 wt pct Nb after cathodic hydrogen charging revealed the precipitation of (Ti,Nb)H_x, thus leading to an $\alpha'' + \beta$ + (Ti,Nb)H_x microstructure. Electron diffraction (Figure 3(d)) obtained from the parallel hydride plates revealed an orthorhombic hydride (Figure 3(e)) with lattice constants close to a = 0.434 nm, b = 0.418 nm, and c = 0.402 nm.

The X-ray as well as electron diffraction (Figure 4(b)) of sintered Ti-40 wt pct Nb exhibited a bcc phase with a lattice parameter of a = 0.331 nm. In addition, some diffuse spots were observed by electron diffraction, which correspond to the hexagonal ω phase.

Until now, the formation of two types of ω phase has been reported in binary titanium and zircon bcc solid solutions:[20] the as-quenched or athermal ω phase, which is formed during quenching from the β-transus temperature, and the aged or isothermal ω phase, which is formed during aging at temperatures between 200 °C and 400 °C of specimens which have been quenched and contain athermal ω phase or the bcc phase. Further X-ray and electron diffraction studies reveal that the ω phase gives sharp reflections at low solute contents, but diffuse reflections at high solute contents.[19] The electron diffraction for the investigated Ti-40 wt pct Nb alloy (Figure 4(b)) showed a diffuse ω phase, which occurs in alloys with high Nb contents.

The storage capacity of Ti-40 wt pct Nb after hydrogenation at 500 A/ m^2 for 24 hours was found to be about 3000 ppm. Hydrogenation led to a shift to lower diffraction angles and higher intensities in the X-ray diffraction and to an increase of the lattice constant after charging at 500 A/ m^2 for up to 24 hours. The influence of hydrogen on the phase stability of sintered Ti-40 wt pct Nb was observed to be very similar to commercial Ti-45 wt pct Nb, which will be explained in detail subsequently.

Optical microscopy as well as SEM studies of the cross section of commercial Ti-45 wt pct Nb rods revealed a "Van Gogh's sky" contrast, which is known, *e.g.*, for B2 aluminides obtained by extrusion.[21] Microstructural investigations of Ti-45 wt pct Nb by X-ray (Figure 5) and electron diffraction (Figure 6(b)) revealed the existence of the bcc

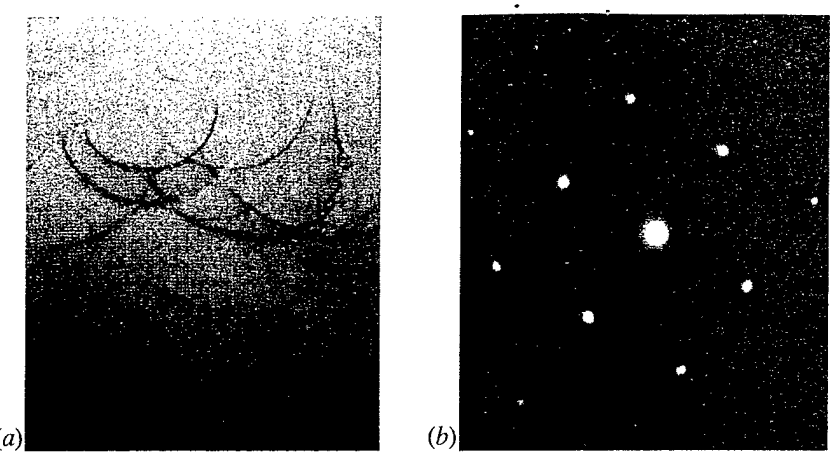

Fig. 4—Microstructure of Ti-40 wt pct Nb: (*a*) TEM bright-field image and (*b*) corresponding electron diffraction pattern of the bcc β phase and the ω hexagonal phase.

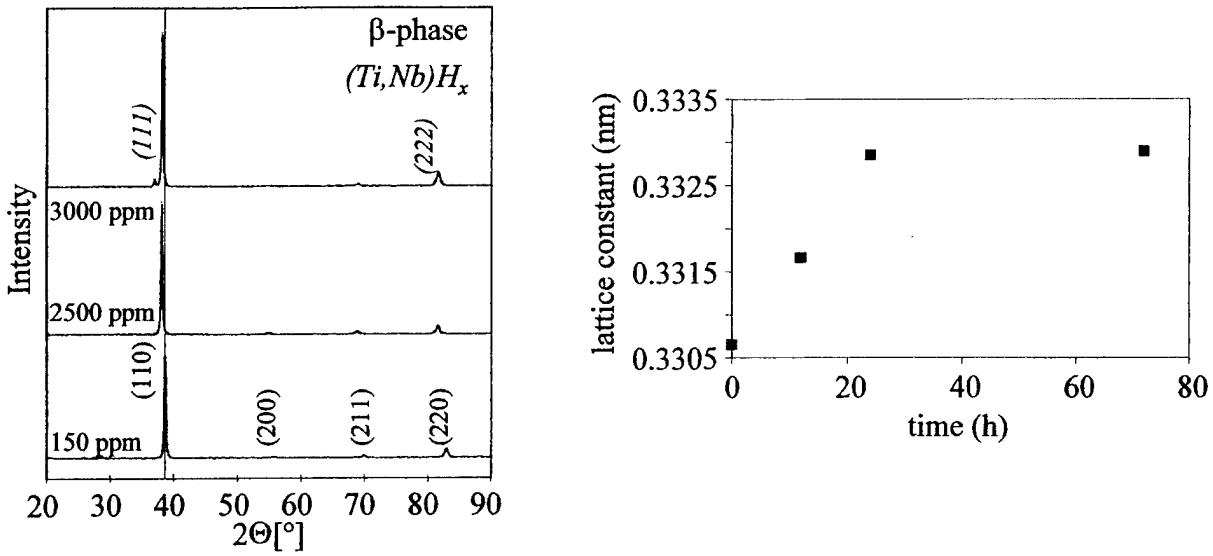

Fig. 5—X-ray diffraction and corresponding change of the lattice parameter of the β phase after hydrogenation.

β phase (a = 0.331 nm). In addition, electron diffraction exhibits some diffuse spots corresponding to the diffuse hexagonal ω phase. The indexed pattern (Figure 6 (c)) reveals the following orientation relationship to the parent β phase: $[110]_\beta$ parallel $[1120]_\omega$.

The hydrogen content in Ti-45 wt pct Nb after hydrogenation at 500 A/m^2 for 24 hours was found to be the same as for Ti-40 wt pct Nb. Cathodic charging led to a shift to lower angles and higher intensities in the X-ray diffraction (Figure 5), *i.e.*, an increase of the lattice constant of about 1 pct. After longer charging, no further increase of the lattice constant occurred, but the formation of (Ti,Nb)H_x (a = 0.434 nm, b = 0.48 nm, and c = 0.402 nm) was observed.

Optical microscopy and SEM studies revealed no change in the microstructure after cathodic charging. Figures 6(d) and (e) show TEM micrographs of Ti-45 wt pct Nb after hydrogenation up to 2500 ppm at 500 A/ m^2 for 12 hours; no evidence for the existence of the phase was found. Although there are very few studies[20] that attempted to explain the occurrence and stability of the ω phase, the results suggest that hydrogen affects the stability of this phase and leads to the dissolution of the metastable hexagonal phase. The TEM studies of Ti-45 wt pct Nb after hydrogenation up to 3000 ppm (500 A/ m^2 for 24 hours), shown in Figures 6(f) and (g), confirms the formation of an orthorhombic (Ti,Nb)H_x.

B. *Effect of Hydrogenation and Deformation on Thermal Desorption*

Thermal desorption analysis of Ti-Nb (20 to 45 wt pct Nb) alloys (Figure 7) showed that desorption of deuterium in these alloys is affected by the niobium content, which influences the phases that are formed. The desorption temperature increases with the niobium content and reaches almost the same peak temperature and half-width for sintered Ti-40 wt pct Nb in comparison to extruded Ti-45 wt pct Nb.

The first thermal-desorption-analysis experiments of sintered Ti-20 wt pct Nb (Figure 8(a)) and Ti-40 pct Nb (Figure 8(b))

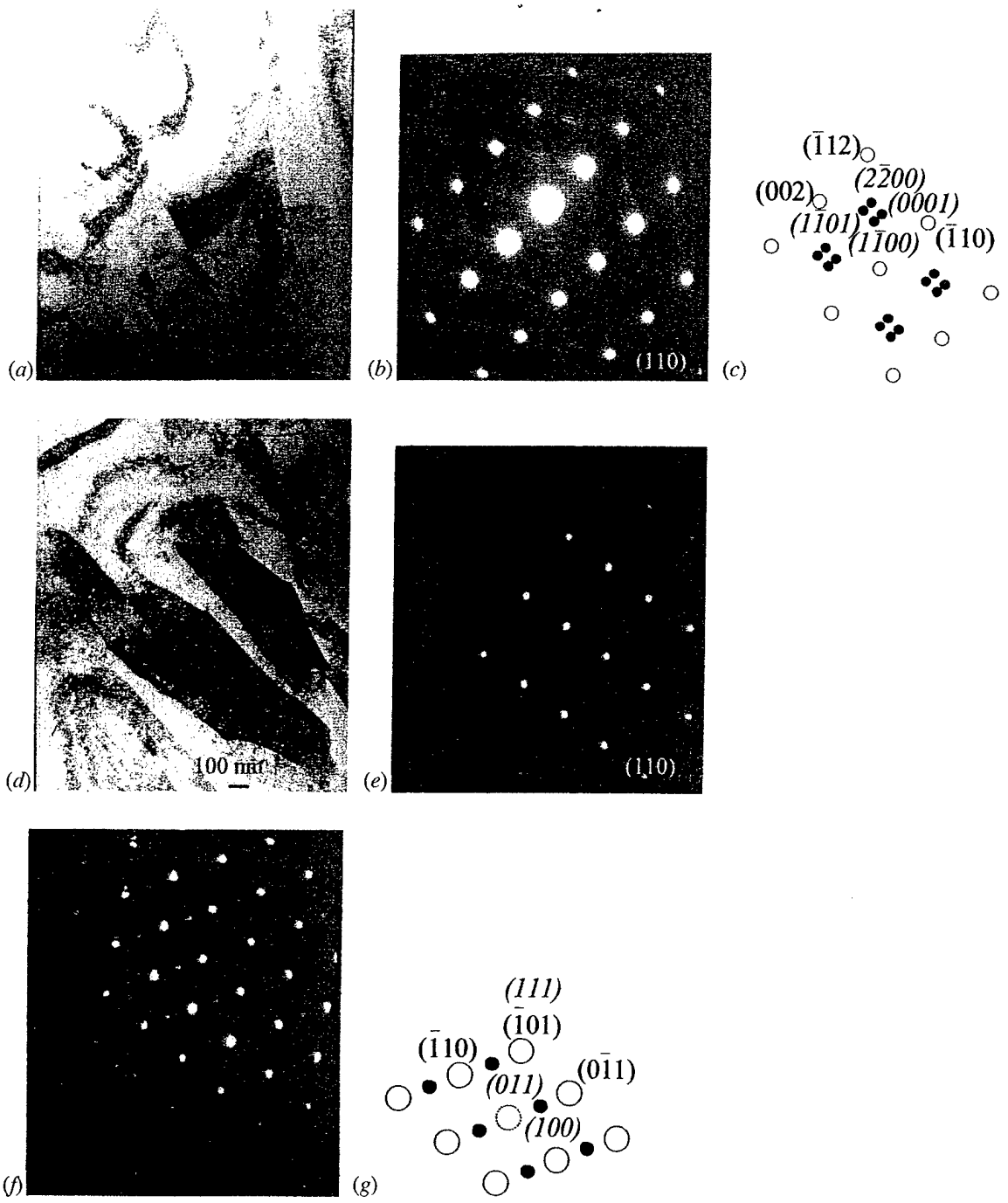

Fig. 6—Influence of hydrogenation on the microstructure of Ti-45 wt pct Nb: (*a*) TEM of the extruded alloy, (*b*) corresponding electron diffraction pattern of the bcc β phase and the hexagonal ω phase, (*c*) index scheme of the electron diffraction of bcc β phase (○) and the hexagonal ω phase (●), (*d*) TEM of the hydrogenated alloy up to 2500 ppm (500 A/m^{2}for 12 h), (*e*) corresponding electron diffraction pattern of bcc β phase, (*f*) electron diffraction pattern of bcc β phase and (Ti,Nb)H_x after charging up to 3000 ppm (500 A/m^2 for 24 h), (*g*) index scheme of the electron diffraction of bcc β phase (○) and the orthorhombic (Ti,Nb)H_x phase (●).

on the influence of deformation showed an increase of the peak temperature after 20 and 40 pct deformation by cold rolling prior to hydrogenation up to 3000 ppm deuterium, as well as a change of the half-width to lower values.

The desorption of deuterium occurred for Ti-20 wt pct Nb after charging and 20 pct deformation at a higher peak temperature and broader temperature range between 360 °C and 550 °C than for undeformed Ti-20 wt pct Nb after hydrogenation. For Ti-40 wt pct Nb, the temperature range for desorption of deuterium seems to be independent of a certain extent of deformation. Further, it was observed that desorption starts at the same temperature of about 360 °C for these two Ti-Nb alloys.

Figure 9 shows the thermal-desorption analysis of extruded Ti-45 wt pct Nb after hydrogenation with deuterium at high fugacities and 20 pct deformation by cold rolling. It was observed that the deformation after hydrogenation decreases the peak temperature as well as the peak intensity.

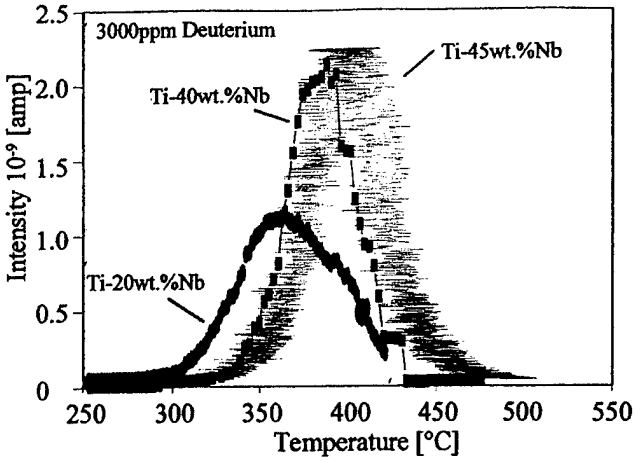

Fig. 7—Thermal desorption analysis (5 K/min) of Ti-Nb (20 to 45 wt pct Nb) after hydrogenation.

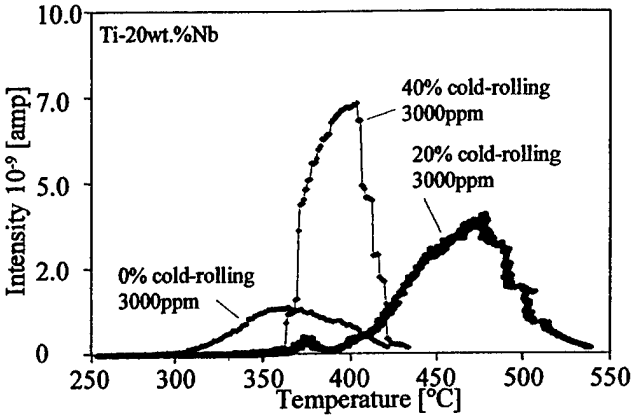

(*a*)

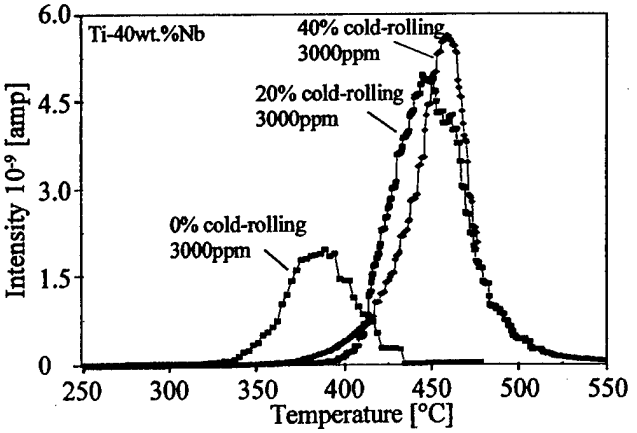

(*b*)

Fig. 8—Thermal desorption analysis (5 K/min) of (a) Ti-20 wt pct Nb and (b) Ti-40 wt pct Nb hydrogenated after deformation.

C. *Effect of Hydrogenation on Microhardness*

Figure 10 shows the influence of hydrogenation on the microhardness of sintered Ti-20 wt pct Nb, Ti-40 wt pct Nb, and extruded Ti-45 wt pct Nb. It is known[22,17] that the microhardness is strongly influenced by the methods used in the production of the alloy, the niobium content, as well as

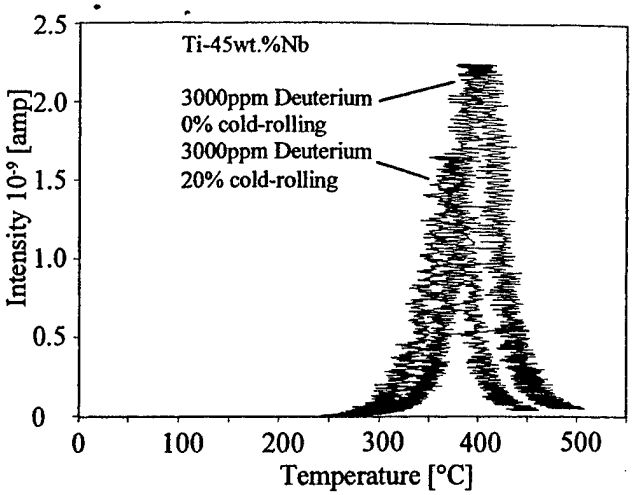

Fig. 9—Thermal desorption analysis (5 K/min) of Ti-45 wt pct Nb20 pct deformed after hydrogenation.

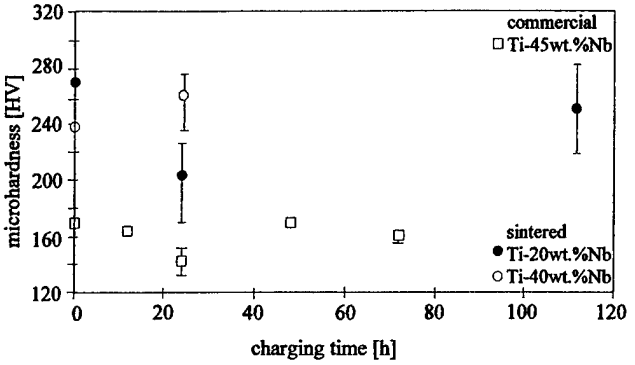

Fig. 10—Influence of hydrogenation on the microhardness of sintered Ti-20 wt pct Nb, Ti-40 wt pct Nb, and extruded Ti-45 wt pct Nb.

the precipitation of metastable α and ω phases. Precipitation of the ω phase, deformation, or alloying with interstitials (for example, hydrogen) is often accompanied by an increase in the hardness.

The microhardness of sintered Ti-20 wt pct Nb was observed to be about 270 HV; that of sintered Ti-40 wt pct Nb was about 240 HV, and that of extruded Ti-45 wt pct Nb was about 170 HV. Popov *et al.*[22] reported a microhardness of about 160 HV for quenched Ti-45 wt pct Nb, and this result fits very well with the examined alloy. However, the microhardnesses of the sintered Ti-Nb alloys (20 to 45 wt pct Nb) used in this investigation differ significantly from the reported values. These differences between our experimentally derived values and those found in literature are likely due to the different fabrication processes.

The microhardness of sintered Ti-20 wt pct Nb decreased significantly in response to hydrogenation for 24 hours at high fugacities (Figure 10), whereas the microhardness shows only minor changes after hydrogenation of sintered Ti-40 wt pct Nb as well as of extruded Ti-45 wt pct Nb.

IV. DISCUSSION

Hydrogen capacity is mainly influenced by the chemical interactions between metal and hydrogen atoms as well as

the number, type, and size of the interstitial sites in the material. The affinity of titanium to hydrogen, the processes of formation and recombination at the electrode, and the following diffusion of hydrogen into the material are the main factors which influence the absorption kinetic. The less-densely packed bcc phase in Ti-Nb (40 and 45 wt pct Nb) allows faster hydrogen diffusion in the investigated β phase in comparison to the orthorhombic α'' phase in the Ti-20 wt pct Nb alloy, even despite the very high affinity of Ti to hydrogen. The faster hydrogen diffusion can explain also the higher hydrogen content after 72 hours for sintered Ti-40 wt pct Nb and extruded Ti-45 wt pct Nb.

Ti-20 wt pct Nb after cathodic hydrogen charging revealed a precipitation reaction which leads to the transformation of $\alpha'' + \beta$ into $\alpha'' + \beta + (Ti,Nb)H_x$. Because of the lower solubility limit of hydrogen in the hcp α phase,[23] hydride plates were more likely to precipitate within the α'' grains. These packets of parallel hydrides within the primary α'' grains resulted from the supersaturation in hydrogen, which diffused into the α'' grains and segregated at the habit planes. In comparison to the observations for hydrogenated Ti-20 wt pct Nb, the precipitation of nanocrystalline $(Ti,Nb)H_x$ was found in Ti-Nb (40 and 45 wt pct Nb).

During hydrogenation, the microhardness might be changed by the interstitial content and microstructural changes, *e.g.*, phase transformations as well as precipitation. The addition of interstitials (*e.g.*, hydrogen) to a Ti-Nb alloy should lead to an increase in hardness. The precipitation of relatively large hydrides should not change the microhardness significantly. However, the *microhardness* of sintered Ti-20 wt pct Nb decreased significantly in response to hydrogenation for 24 hours at high fugacities. As described earlier, cathodic hydrogen charging causes the precipitation reaction of $(Ti,Nb)H_x$ in consumption of α''in the α'' and β microstructure. Since the α'' phase exhibits a higher hardness than the β phase, such a reaction will lead to softening due to an increased ratio of α''/β.

For hydrogenated sintered Ti-40 wt pct Nb as well as extruded Ti-45 wt pct Nb, the microhardness measurements show only minor changes with the hydrogen content. It might be that the minor change of the microhardness in Ti-45 wt pct Nb is due to a partial superimposition of the destabilization of the ω phase causing a softening of the β phase during hydrogen charging and an increase in hardness due to the interstitial hydrogen in the β phase.

The TDS tests were done in order to analyze the influence of the microstructure on hydrogen desorption and, in detail, the influence of the phases present, depending on the niobium content and the influence of deformation either or after hydrogenation.

The desorption of deuterium is influenced by the microstructure as well as the depth of trapping sites. Desorption of deuterium in Ti-Nb (20 to 45 wt pct Nb) proceeds with increasing niobium content at higher temperatures. It seems reasonable that the present phases are the dominant factors for the different desorption behaviors, since the formation of the orthorhombic α'' phase in Ti-20 wt pct Nb as well as the formation of the bcc β phase in Ti-Nb (40 and 45 wt pct Nb) strongly depend on the niobium content and the cooling rate. To the authors' knowledge, thermodynamic data on the stability of these phases are not available. It also has to be considered that the formation of a hydride already at a deuterium content of 3000 ppm for all investigated alloys was observed; $(Ti,Nb)H_x$ precipitates as parallel plates in the α'' phase, but as nanocrystalline particles in the bcc phase.

As already mentioned, the less-densely packed bcc phase allows faster diffusion of hydrogen or deuterium in comparison to the orthorhombic α'' phase; this behavior would explain the narrower half-width for Ti-Nb with 40 as well as 45 wt pct niobium. Since in both phases no channeling of deuterium was observed until now, this parameter will not cause a difference in the desorption behavior. In addition, a localized decomposition of hydride plates necessary in Ti-20 wt pct Nb could result in larger diffusion distances and, therefore, a longer desorption time for deuterium and a broader desorption peak than in the bcc Ti-Nb alloy with nanosized particles.

The lower peak temperature of sintered Ti-20 wt pct Nb might also be explained by a higher porosity and/or voids in the alloy due to the fabrication process. The similar desorption behavior of sintered Ti-40 wt pct Nb and extruded Ti-45 wt pct Nb, on the other hand, indicates a very similar and dense material. The SEM investigations of the sintered Ti-20 wt pct Nb and Ti-40 wt pct Nb confirmed this assumption.

The influence of a higher dislocation density on deuterium desorption was studied after deformation prior to deuterium charging. Investigations of sintered Ti-20 wt pct Nb and Ti-40 wt pct Nb showed an increased desorption temperature, thus indicating a change of the trapping sites and transport mechanism of hydrogen in the deformed microstructure (20 pct cold rolled) to higher trapping-energy values due to the deformation and/or deuterium segregation at dislocation cores.

In Ti-20 wt pct Nb, however, a further increase of the deformation rate by cold rolling from 20 to 40 pct did not result in a further increase of the desorption temperature, but a significant decrease. This surprising behavior is not understood at the moment. There might be microstructural changes due to the deformation. Or, one might assume that the higher dislocation density hinders any hydride formation, thus leading to a significant change in the mode of hydrogen storage.

Deuterium charging followed by deformation of extruded Ti-45 wt pct Nb leads to a reduced desorption temperature. One has to compare this behavior with the opposite shift observed in sintered Ti-40 wt pct Nb after 20 pct deformation prior to charging. The first X-ray and TEM investigations of Ti-45 wt pct Nb showed that the same phases are present, in the hydrogenated as well as in the hydrogenated and deformed alloy.

As already mentioned, deformation prior to deuterium charging will lead to a stronger interaction between defects, in particular, dislocation and the hydrogen. Defects generated in an already hydrogenated alloy do not exhibit this behavior. It is known that hydrogenation of β itanium[24] prior to deformation leads to an increased percentage of screw dislocations, thus leading to a lower desorption temperature due to the reduced trapping energy.

Further experiments and detailed microscopic investigations should provide a better knowledge of the interaction between titanium and hydrogen as well as between hydrogen and dislocations in the different microstructures available in Ti-Nb alloys, thus leading to an improved understanding of the use of hydrogen as a temporary alloying element.

V. CONCLUSIONS

The studies of sintered Ti-20 wt pct Nb and Ti-40 wt pct Nb, as well as of commercial Ti-45 wt pct Nb, showed a strong influence of hydrogen at high fugacities on the phase stability and microhardness as well as on the thermal desorption of the hydrogenated Ti-Nb alloys which were deformed before or after deuterium charging.

It was observed that hydrogenation of Ti-20 wt pct Nb led to the transformation of $\alpha'' + \beta$ into $\alpha'' + \beta$ $(Ti,Nb)H_x$. The intensities of the X-ray peaks of the bcc phase are much higher and less diffuse after electrochemical hydrogenation than before. It was assumed that because of the lower solubility limit of hydrogen in the α phase, hydride plates were more likely to precipitate within the α'' grains.

The microhardness of sintered Ti-20 wt pct Nb decreased significantly during hydrogenation at high fugacities. The observed softening might occur due to a change in the α''/β ratio during the precipitation of $(Ti,Nb)H_x$, as mentioned previously.

Microstructural investigations of Ti-40 wt pct Nb and Ti-45 wt pct Nb alloys reveal the bcc β phase as well as the diffuse ω phase. Cathodic hydrogen charging leads to stabilization of the bcc phase, but to destabilization of the hcp ω phase. An expansion of the lattice constant of the β phase and the formation of $(Ti,Nb)H_x$ could be observed in Ti-45 wt pct Nb.

The microhardness showed only a minor change after hydrogenation for Ti-40 wt pct Nb and for Ti-45 wt pct Nb alloys. It is assumed that the minor decrease of the microhard-ness in Ti-45 wt pct Nb is due to the destabilization of the ω phase during hydrogen charging and the following increase due to the precipitation of $(Ti,Nb)H_x$.

Thermal desorption analysis showed that desorption of deuterium in Ti-Nb (20 to 45 wt pct Nb) is influenced by the niobium content, more probably by the phases present. The desorption temperature increases with the niobium content.

Deformation prior to deuterium charging led to an increased desorption temperature. One explanation for this influence could be that trapping sites formed during the deformation have a stronger affinity for deuterium and/or deuterium segregates at dislocation cores.

Deuterium charging followed by deformation of Ti-45 wt pct Nb, however, leads to a reduced desorption temperature, probably due to an increased amount of screw dislocations generated during the deformation of the hydrogenated β phase.

ACKNOWLEDGMENTS

The authors acknowledge the research support of the United States Army Research Office and the Ben-Gurion University of the Negev. The authors thank Professor U. Köster (Department of Chemical Engineering, University of Dortmund, Dortmund, Germany) for fruitful discussions.

REFERENCES

1. H. Fujii: *Mater. Sci. Eng.*, 1998, vol. A243, p. 103.
2. F.H. Froes and D. Eylon: in *Hydrogen Effect on Material Behavior*, N.R. Moody and A.W. Thompson, eds., TMS, Warrendale, PA, 1990, p. 261.
3. F.H. Froes, D. Eylon, and C. Suryanarayana: *JOM*, 1990, vol. 42, p. 26.
4. F.H. Froes, D. Eliezer, and H.G. Nelson: *Proc. 5th Int. Conf. on Effects of Hydrogen Behavior of Materials*, 1994, N.R. Moody and A.W. Thompson, eds., TMS-AIME, Warrendale, PA, 1996, p. 719.
5. W.R. Kerr: *Metall. Trans.*, 1985, vol. 16A, pp. 1077-87.
6. J. Greenspan, F.J. Rizzitano, and E. Scala: in *Titanium, Science and Technology*, R.I. Jaffee and H.M. Burke, eds., Plenum Press, New York, NY, 1973, vol. 1, p. 365.
7. W.R. Kerr, P.R. Smith, M.E. Rosenblum, F.J. Gurney, Y.R. Mahajan, and L.R. Bidwell: in *Proc. 4th Int. Conf. Titanium*, Kyoto, Japan, H. Kimura and O. Izumi, eds., AIME, Warrendale, PA, 1980, p. 2477.
8. U. Zwicker: U.S. Patent No. 2,892,742, June 1959.
9. H.J. Goldschmidt: *Interstitial Alloys*, Butterworth, and Co. London, 1967, p. 445.
10. H. Kimura, H. Matsui, A. Kimura, T. Kimura, and K. Oguri: *Proc. 3rd Int. Conf. on Effects of Hydrogen on Behavior of Materials* 1980, I.M. Bernstein and A.W. Thompson, eds., TMS-AIME, Warrendale, PA, 1981, p. 191.
11. A.A. Popov, A.A. Il'in, M.Y. Kollerov, A.G. Illarionov, and E.O. Agarkova: *Metals*, 1994, vol. 5, p. 109.
12. A.A. Popov, A.G. Illarionov, S.L. Demakov, and O.A. Elkina: *Int. J. Hydrogen Energy*, 1997, vol. 22, p. 195.
13. E. Abramov and D. Eliezer: *Metall. Mater. Trans. A*, 1994, vol. 25A, pp. 949-59.
14. E. Abramov and D. Eliezer: *Proc. 5th Int. Conf. on the Effect of Hydrogen on the Behavior of Materials*, A.W. Thompson and N.R. Mopdy, eds., TMS, Warrendale, PA, 1996, p. 293.
15. K.L. Wilson and M.I. Baskers: *J. Nucl. Mater.*, 1978, vols. 76-77, p. 291.
16. G. Farrel and G. Carter: *Vacuum*, 1967, vol. 17, p. 15.
17. T. Ahmed and H.J. Rack: *J. Mater. Sci.*, 1996, vol. 31, p. 4267.
18. A.R.G. Brown and K.S. Jepson: *Mem. Sci. Rev. Metall.*, 1966, vol. 63, p. 575.
19. D.L. Moffat and D.CC. Larbalestier: *Metall. Trans. A*, 1988, vol. 19A, pp. 1677-86.
20. S.L. Sass: *J. Less-Common Met.*, 1972, vol. 28, p. 157.
21. S. Naka, M. Marty, M. Thomas, and T. Khan: *Mater. Sci. Eng.*, 1995, vols. A192-A193, p. 69.
22. A.A. Popov, A.A. Il'in, A.G. Illarionov, O.A. Elkina, and M.Y. Kollerov: *Phys. Met. Metallogr.*, 1994, vol. 78, p. 204.
23. H. Numakura and M. Koiwa: *Acta Metall.*, 1984, vol. 32, p. 1799.
24. D.F. Teter, I.M. Robertson, and H.K. Birnbaum: *Acta Mater.*, 2001, vol. 49, p. 4313.